https://doi.org/10.4467/21995923GP.24.005.20472 GEOINFORMATICA POLONICA
23: 2024

Prashant Patil[1,2]
https://orcid.org/0000-0002-1256-0326

Chidanand Patil[4]
https://orcid.org/0000-0001-5820-7803

Shravankumar Musalvad[5]
https://orcid.org/0000-0002-4492-9618

Nagaraj Hegde[1]
https://orcid.org/0000-0002-4104-657X

Uttam Kumar Sahoo[1]
https://orcid.org/0000-0002-6524-1775

Satish Tarekodlu Janardhana[3]
https://orcid.org/0009-0006-5368-7485

Suresh Kumar[1]
https://orcid.org/0000-0003-1081-3040

Nicolee Lyngdoh[6]
https://orcid.org/0000-0001-5900-2914

MONITORING LAND USE LAND COVER CHANGE AND ITS IMPACT ON CLIMATIC PARAMETERS USING REMOTE SENSING AND GIS: A CASE STUDY OF LOWER DIBANG VALLEY, ARUNACHAL PRADESH, INDIA

[1] Department of Forestry, Mizoram University, Aizawl-796004, Mizoram, India
[2] Renew Power Synergy Private Limited, Gurugram-122009, Haryana, India
ptpatil@hotmail.com
[3] Capacity Building Commission, DOP&T, New Delhi-110001, India
satishtj.dad@gov.in
[4] Department of Civil Engineering, Dr. M. S. Sheshgiri College of Engineering and Technology, Udyambagh, Belagavi-590008, India
chidu.patil@gmail.com
[5] Department of Civil Engineering, Sreenidhi Institute of Science and Technology Hyderabad Telangana-501301, India
shravankumarsm@sreenidhi.edu.in
[6] BiodiversityResearch Centre, Mizoram University, Aizawl-796004, Mizoram, India
lyngdoh@gmail.com

Abstract

The changes in the socio-dynamics and the pattern of occurrences of natural hazards both at larger and regional scales have been influenced by the alterations in the Land use land cover change (LULCC) modifications. The LULCC of Lower Dibang valley of Arunachal Pradesh is investigated using contemporary tools of Remote sensing and Geographic Information system. A temporal analysis is done for the years viz, 2009, 2014, and 2021 using USGS Landsat satellite images. To determine the change in

LULCC support vector machine a supervised classification method is used and is cross checked with Google Earth points for achieving accuracy and the temporal analysis is done by comparing each images pixel by pixel. The findings show that between 2009 and 2021, the region had significant changes in land cover in the following areas: forest area (–8%), rangeland/scrubland (–6%), barren land/bare soil/open rocks (–1%), agricultural (-2%), and water body/river (–1%). It was observed that lowland and higher altitude regions saw the majority of the LULCC alterations. In the seven tehsils of the Lower Dibang Valley of Arunachal Pradesh, which are located at varying elevations and slopes, the effects of LULC changes on climatic and environmental variables such as latent/sensible heat flow, temperature, precipitation, and specific humidity have been evaluated independently. This research paper's methodology and results section includes a full explanation of the procedures followed and the outcomes.

Keywords: Land use land cover (LULC), machine learning, Landsat-8, change detection

MONITORING ZMIAN UŻYTKOWANIA I POKRYCIA TERENU ORAZ ICH WPŁYWU NA PARAMETRY KLIMATYCZNE PRZY UŻYCIU TELEDETEKCJI I GIS: STUDIUM PRZYPADKU W DOLINIE DOLNY DIBANG, ARUNACHAL PRADESH, INDIE

Abstrakt

Na zmiany socjodynamiki i wzorca występowania naturalnych zagrożeń zarówno w skali regionalnej, jak i większej mają wpływ modyfikacje użytkowania i pokrycia terenu (ang. *land use land cover change* – LULCC). Wskaźnik LULCC w Dolinie Dolny Dibang w Arunachal Pradesh badano przy użyciu nowoczesnych narzędzi teledetekcyjnych oraz Geograficznego Systemu Informacji (GIS). Analizę zmian w czasie przeprowadzano dla lat 2009, 2014 i 2021 przy pomocy zobrazowań satelitarnych USGS Landsat. Aby określić zmiany w LULCC zastosowano maszynę wektorów nośnych, metodę klasyfikacji nadzorowanej, którą skonfrontowano z punktami w Google Earth, aby osiągnąć dokładność, a analizy zmian w czasie dokonano porównując każdy obraz piksel po pikselu. Wyniki pokazują, że pomiędzy rokiem 2009 i 2021 region ulegał znaczącym zmianom pokrycia terenu w następujących aspektach: zalesienie (–8%), pastwiska/zarośla (–6%), ogołocona ziemia/gołe skały (–1%), obszary rolnicze (–2%) oraz zbiorniki wodne/rzeki (–1%). Zaobserwowano, że większość zmian LULCC wystąpiła na nizinach i większych wysokościach. W siedmiu tehsilach (jednostka administracyjna) Doliny Dolnego Dibangu (Arunachal Pradesh) położonych na różnych wysokościach i stokach niezależnie oceniono skutki zmian LULC w odniesieniu do parametrów klimatu i środowiska, takich jak przepływ ciepła utajonego/jawnego, temperatura, opady oraz wilgotność właściwa. Rozdziały pracy przedstawiające metodykę i wyniki w pełni objaśniają użyte procedury i otrzymane rezultaty.

Słowa kluczowe: użytkowanie i pokrycie terenu (LULC), uczenie maszynowe, Landsat-8, wykrywanie zmian

1. INTRODUCTION

The anthropogenic intervention across the different subsystems of the earth is responsible for severe changes in the land use land cover, which alter ecosystems, thus it is imperative to continuously monitor the changes occurring in the LULCC [1, 2, 3, 42, 43]. LULCC changes may contribute to the increase of land surface temperature and thereby may enhance formation and intensity of urban heat islands [4, 44, 45]. In the Eastern Himalayas shifting cultivation, and conversion of land for commercial plantations, such as oil palm, areca nut, rubber, etc., have been the major forces for rapid LULCC. In some regions, both forest and agricultural lands have shown a decline due to urbanization and mushrooming of aquaculture [5, 46]. The anthropogenic factor for the evolution of the mankind has been responsible for the consequences of LULCC [6, 47, 48]. The rapid economic growth of developing countries backed by their large working population has boomeranged the LULCC in the recent years and has altered the niche of basic vital sources of life viz., vegetation, soil and water [7, 8, 49]. The study of impact of LULCC should not be restricted spatially and temporally to local scale; on the contrary, the effects must be studied on a global scale [13, 14, 50].

To understand the changes in natural resources the stake holders and decision makers should understand the changes taking place in LULCC [15, 51], hence a thorough study of changes in LULC is necessary to make a wise and effective decision. The biotic and abiotic processes on earth are being influenced and affected

due to changes in LULCC according to many empirical studies [17, 18, 47]. The contemporary problems associated with that of global warming and climate change have been linked to LULCC, beb0ming the epicentre of geopolitics, which has emphasised the study of change detection of LULC [14, 19, 20, 52]. The continuous monitoring of environmental degradation requires systematic assessment of LULCC which can be used as evidence for assessing the impact both spatially and temporally [22, 47, 11, 21].

To obtain the best or the most efficient classified image that provides supreme LULC information, the process must defy many challenges viz., the heterogeneity of landscape, the satellite images pre-processing labour to retrieve maximum information with minimum error corrections and choosing the reliability indices for the classified images. The most popular parametric classifier, maximum likelihood decision rule, and a few ancillary data, including locality knowledge, land use data, vegetation index, and textural analysis of the Landsat images that can be used for in-depth post-classification change detection, have been used to classify Landsat TM data over the past year to achieve improvement [23, 24, 53].

The Indian Eastern Himalayas are undergoing tremendous forest degradation owing to frequent forest fires [25], indiscriminate deforestation and shifting cultivation [26], as well as land use changes [27–29]. Though at a few sporadic places in the region there is a decrease in shifting cultivation area owing to socioeconomic development [30–32, 46], anthropogenic activities continue to rise causing loss of biodiversity [33], disruption of ecosystem function, regional climate, and people's life and livelihood [34, 35, 52]. A study in Nagaland indicated a decline in both forest and agricultural lands due to urbanization and practices of aquaculture [5].

Some efforts have been done to identify LULC change in the eastern Arunachal Pradesh from1985 to 2005 [36], and LULC mapping of Mouling National Park [37], but no recent quantified data on LULC changes is available. Lower Dibang Valley is of greater importance to the region due to several reasons. The district rises from the Himalayan foothills to the middle ranges with the highest point of Mayudia at the height of 2655 meters from mean sea level. Snow-capped peaks, turbulent rivers, mystic valleys, and abundance of rich flora and fauna are attractions of the district. The district is well known for its largest cover of thick green forest with almost 80% of the area being notified as reserved forest, wildlife sanctuaries, or unclassified state forests (https://roing.nic.in/about-district). Therefore, the identification of various LULC will not only provide baseline information, but the decadal change monitoring will contribute to regional planning, effective land use management, and conservation initiatives.

The change in LULC have small to large impacts on the climate cycle. The systematic study and understanding of the changes occurring in LULC and their relations with the environment will contribute to timely and improved management of croplands, forests, grasslands, wetlands, mangroves and water resources. The rapid growth of human population promotes the fast growth of industries and urbanization due to which LULC changes are frequently observed in developing countries such as India. Much research needs to be conducted in this field. However, few studies investigated the countrywide LULC changes and their interactions with energy fluxes and precipitation. In this research paper, LULC changes in Lower Dibang valley of Arunachala Pradesh from 2009 to 2021 have been evaluated by utilizing Landsat ETM and Landsat-8 satellite datasets. The latent, sensible heat fluxes, temperature, precipitation, specific humidity were obtained from the Climate Engine web-based platform (https://app.climateengine.org/climateEngine).

The present study was formulated based on a hypothesis that forest land has declined over the years due to increasing population pressure as well as climate change. With this background, the objectives of the study were to (a) understand the decadal changes in LULC and (b) identify the major anthropogenic factors contributing to LULC changes, (c) understand the effects of LULC on climatic and environmental variables like precipitation, maximum temperature, specific humidity, latent and sensible heat fluxes in 7 tehsils of Lower Dibang valley.

2. MATERIALS AND METHODS

2.1. Study Area

The Lower Dibang Valley district is an administrative district in the state of Arunachal Pradesh in north-eastern India (Fig. 1). The district is rich in wildlife. Rare mammals such as the Mishmi takin (*Budorcas taxicolor taxicolor*), red goral *(Naemorhedus bai-*

leyi), elephants (*Elephas maximus*), wild water buffalo (*Bubalus arnee*), and leaf muntjac (*Muntiacus putaoensis*) and Mishmi Hills giant flying squirrels (*Petauristami shmiensis*) live in the district. Birds that live in the Lower Dibang Valley include Sclater's monal (*Lophophorus sclateri*), Blyth's tragopan (*Tragopan blythii*), the rufous-necked hornbill (*Aceros nipalensis*), the Bengal florican (*Houbaropsis bengalensis*), and the white-winged wood duck (*Asarcornis scutulata*). In 1980, the Lower Dibang Valley district became home to the Mehao Wildlife Sanctuary, which has an area of 282 km^2 (108.9 sq mi). A new subspecies of hoolock gibbon (*Hoolock hoolock*) has been discovered in this area, which was named the Mishmi Hills hoolock.

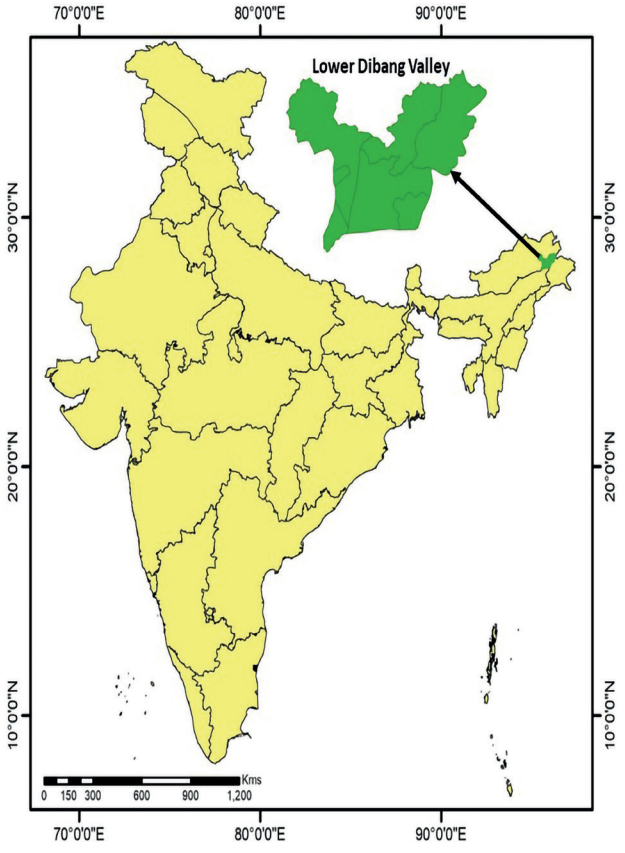

Fig. 1. The location of the study area
Ryc. 1. Lokalizacja obszaru badań

2.2. Methodology

The methodology and procedure employed in the LULC mapping and change detection included interpretation and analysis of current and past satellite images, preliminary land use and land cover classification and mapping, field and signature data collection and verification. During pre-fieldwork, the images were rectified and enhanced to create a more realistic representation of the scene and land cover signatures. Geospatial data uncertainty resulted from image resampling, percent cloud cover, assumptions of homogeneity, and physical properties of the feature of interest were improved by applying geometric and radiometric corrections. The nearest neighbour resampling method was employed, and colour balance or contrast stretching was used for image enhancement through histogram equalization.

2.2.1. Image Downloading and Pre-Processing

Landsat TM and Landsat-8 (path 134,135 row 40, 41) were used in this study. The Landsat TM, and Landsat-8 images of 2009, 2014, and 2021 were downloaded from the GLOVIS site (https://glovis.usgs.gov/app?fullscreen=1). The dates of all 3 images were chosen to be as close as possible to the same vegetation season i.e. November and the first week of December. Landsat TM and Landsat-8 are of 30 m spatial resolution. All visible and infrared bands (except the thermal infrared) were included in the analysis. Remote sensing image processing was performed using Q-GIS software. The training points for various LULC classes are gathered from the ground, with the exception of 2009 and 2014, when they were gathered from Google Earth Pro. For the year 2021, training points were re-collected from the ground.

Image processing involves the manipulation and interpretation of digital images. Radiometric enhancement, however, improved the area image classification by addressing stripping and banding errors that occur when the detector goes out of adjustment. In addition, principal component analysis improved the image visualization with the technique of data compression to produce uncorrelated output bands, segregate noise components, and reduce the dimensionality of data sets.

2.2.2. Classification and Land Cover Mapping

Several classification techniques have been established to extract vital information from imageries. In this study, we primarily used the pixel-based method of supervised classification, i.e. maximum likelihood classification. It is one of the furthermost collective satellite image classification algorithms applied in this

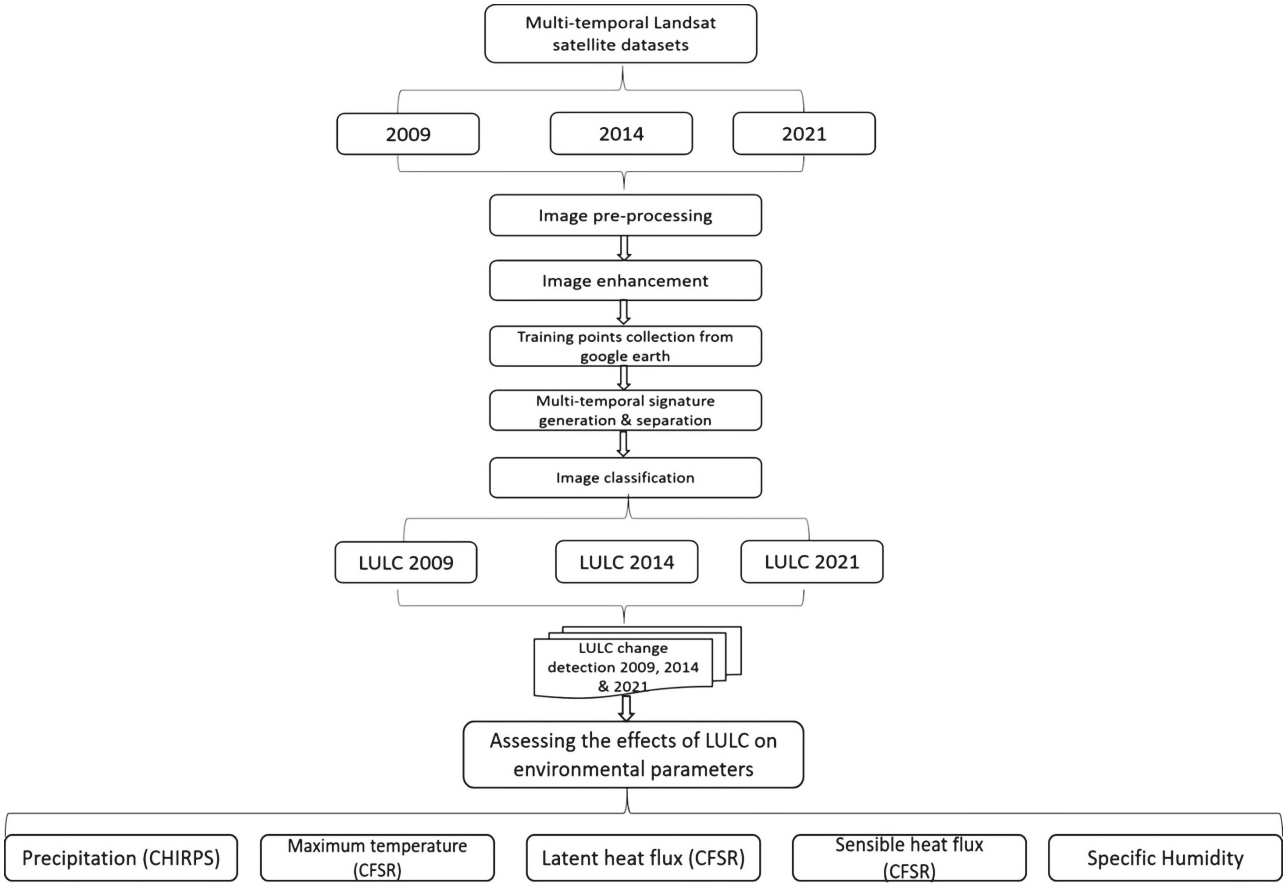

Fig. 2. Flow chart showing the methodology followed in the study
Ryc. 2. Schemat pokazujący zastosowaną w pracy metodykę

study that traces a possibility compactness function and predicts the probability with which a precise pixel fits a specific class. Higher deviations from the centre point will be permissible wherever a pixel is not in the area of a disputing category. The supervised classification techniques work with the discriminant role to allocate the pixel to the class with the maximum probability. Respectively image pixel fits the land cover class aimed at which they become the maximum membership likelihood ensuing the Gaussian normal distribution function. Though the maximum likelihood classification is gentle in computation; yet it is a more accurate statistical decision criterion in classifying the overlapping signatures. In this study, five LULC classes were established as rangeland/scrub land, barren land/bare soil, croplands, forest area, and river/water bodies. A supervised classification technique was used to compare Landsat images from three unique time-period. With this method, these images of different dates are classified independently. Accurate classifications are imperative to ensure precise change-detection results. The detailed steps followed for the study are shown in Fig. 2.

2.2.3. Environmental Data from the Year 2009 to 2021

The effect of LULC change on different key environmental factors like precipitation, maximum temperature, specific humidity, latent and sensible heat fluxes referring to the 7 tehsils of Lower Dibang Valley has been studied by using the time series trends from 2009 to 2021. The trends have been plotted by using the web-based platform climate engine (https://app.climateengine.org/climateEngine). The platform offers different remote sensing and climatic datasets. For all the environmental parameters the timeline considered for the datasets/trends was from the year 2009 to 2021. To study the trend of precipitation we used CHIRPS-4.8km

daily dataset, the unit was in millimeters, the statistic (over day range) was in total and the calculation was of the values. To study the trend of temperature we used CFS-19.2km/28.28km daily dataset, the variable was maximum temperature, the unit was in deg C, the computation resolution (scale) was 19200 (1/5-deg), statistics over region was maximum of the pixel. To study the trend of specific humidity we used CFS-19.2km/28.28km daily dataset the computation resolution (scale) was 19200m (1/5-deg), statistics over the region was mean of the pixel. To study the trend of latent heat flux we used CFS-19.2 km/28.28km daily dataset, the variable was latent heat flux, the computation resolution (scale) was 19200m (1/5-deg), statistics over the region was mean of the pixel. To study the trend of sensible heat flux we used CFS-19.2 km/28.28km daily dataset, the variable was sensible heat flux, the computation resolution (scale) was 19200m (1/5-deg), statistics over the region was mean of the pixel (table-2).

3. RESULTS

3.1 Land Use/Land Cover Classification Map of 2009, 2014 and 2021

The LULC map of 2009 has been generated using 2009 Landsat-5 satellite data (Fig. 3). The LULC classes of 2009 are as follows; forest area is 398 472.8 ha, rangeland/scrubland is 49 839.4 ha, barren land/bare soil/open

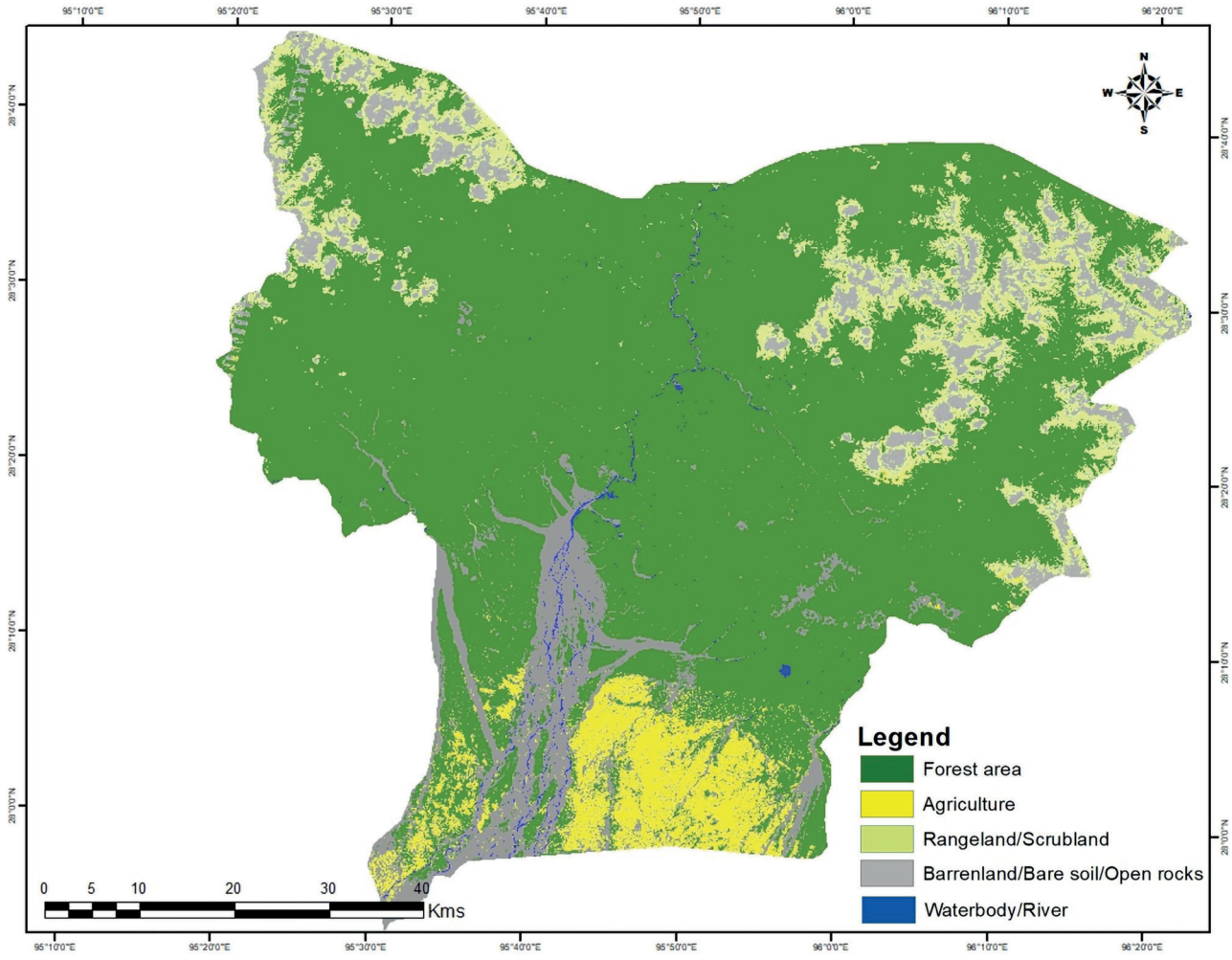

Fig. 3. LULC map of the year 2009
Ryc. 3. Mapa pokrycia terenu (LULC) za rok 2009

rocks are 77 460.33 ha, agriculture is 30 199.13 ha, waterbody/river is 1 868.55 ha.

The LULC map of 2014 has been generated using 2014 Landsat-8 satellite data (Fig. 4). The LULC classes of 2014 are as follows; forest area is 410 846.04 ha, rangeland/scrubland is 33 840.7 ha, barren land/bare soil/open rocks are 58 808.7 ha, agriculture is 52 096.9 ha, water body/river is 2 247.8 ha.

The LULC map of 2021 has been generated using 2021 Landsat-8 satellite data (Fig. 5). The LULC classes of 2021 are as follows; forest area is 351 590.8 ha, rangeland/scrubland is 84 686.2 ha, barren land/bare soil/open rocks are 74 493.7 ha, agriculture is 43 777.1 ha, water body/river is 3 292.5 ha (Fig. 5). The detailed area statistics of the LULC areas have been given in table 1.

3.2. Lulc Changes Trend from 2009, 2014 and 2021

The change detection analysis showed that in the forest class from 2009 to 2014 the area got increased by 2% and in 2021 the area got decreased by 10% compared to 2014 and got decreased by 8% compared to 2009. In the rangeland/scrubland class from 2009 to 2014, the area got decreased by 3% and in 2021 the area got increased by 8% compared to 2014 and the area got increased by 5% compared to 2009. In the barren land/bare soil/open rocks class from 2009 to 2014, the area got decreased by 2% and in 2021 the area got increased by 3% compared to 2014 and increased by 1% compared to 2009. In agriculture class from 2009 to 2014, the area got increased by 2% and in 2021 the area got

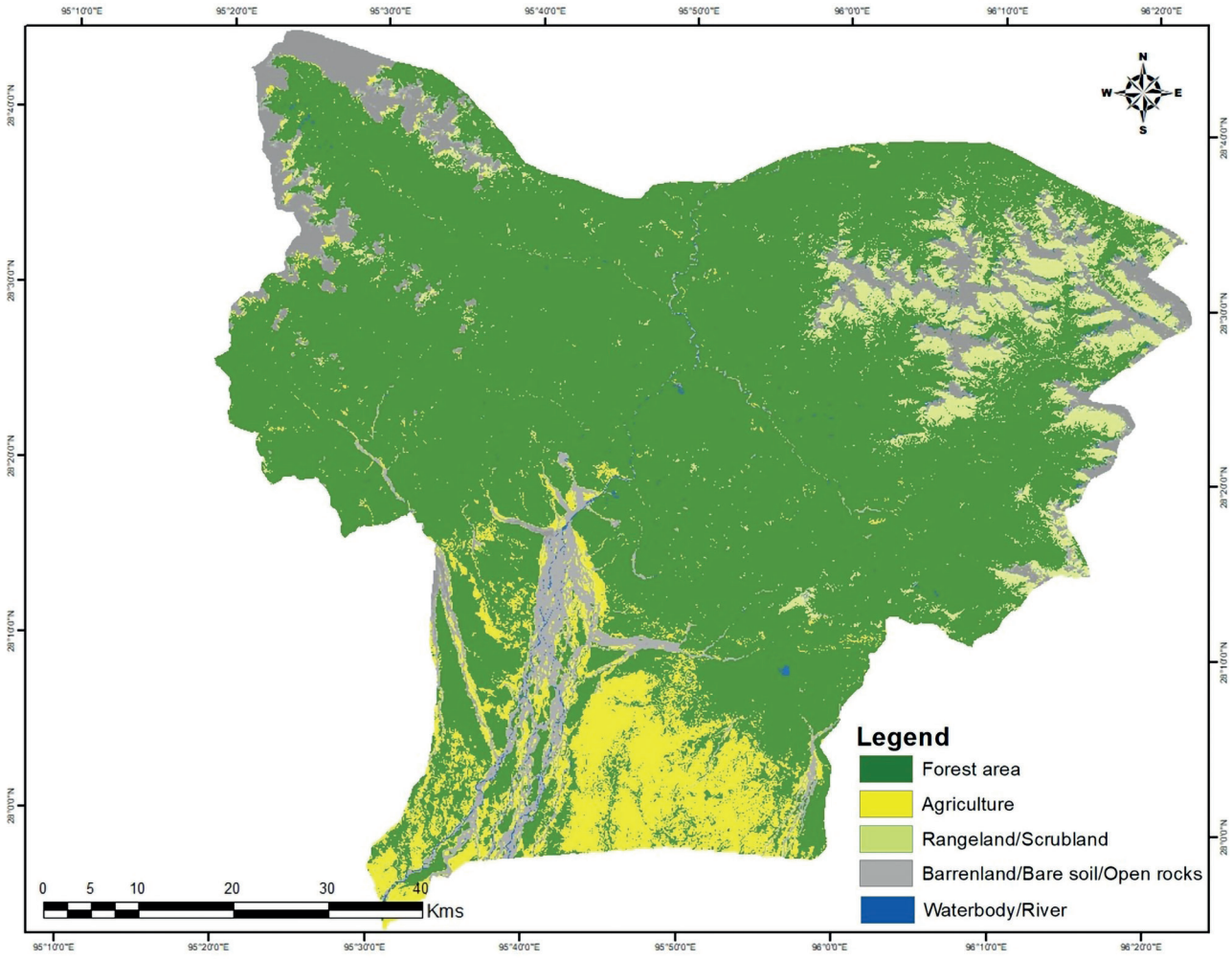

Fig. 4. The LULC map of the year 2014
Ryc. 4. Mapa LULC za rok 2014

Table 1. The trend of areas under different LULC classes of 2009, 2014 and 2021
Tabela 1. Kierunek zmian powierzchni w różnych klasach LULC w 2009, 2014 i 2021 r.

Sl no.	Classes	2009 (ha)	2009 (%)	2014 (ha)	2014 (%)	2021 (ha)	2021 (%)	Changes (%)	Trend
1	Forest area	398472.8	71	410846	73	351590.8	63	(-8)	Declined
2	Rangeland/Scrubland	49839.4	F	33840.7	6	84686.2	14	(+5)	Increased
3	Barren land/Bare Soil/open rocks	77460.3	12	58808.7	10	74493.7	13	(+1)	Increased
4	Agriculture	30199.1	7	52096.9	9	43777.1	8	(+1)	Increased
5	Waterbody/River	1868.6	1	2247.8	2	3292.5	2	(+1)	Increased

decreased by 1% compared to 2014 and increased by 1% compared to 2009. In the water body/river class from 2009 to 2014, the area got increased by 1% and in 2021 the area was the same as compared to 2014 and got increased by 1% compared to 2009 (Fig. 6). The detailed results have been given in table 1.

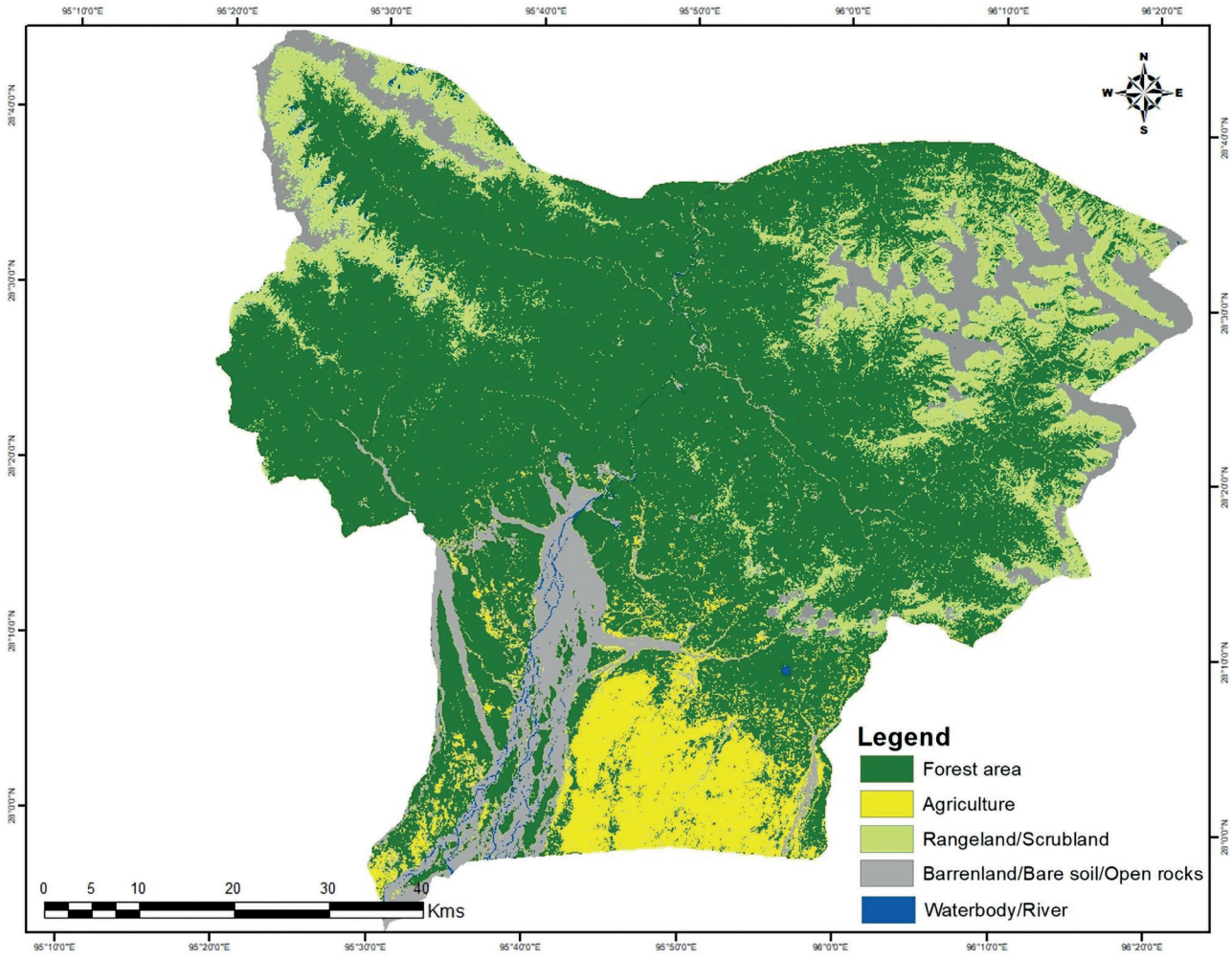

Fig. 5. The LULC map of the year 2021
Ryc. 5. Mapa LULC za rok 2021

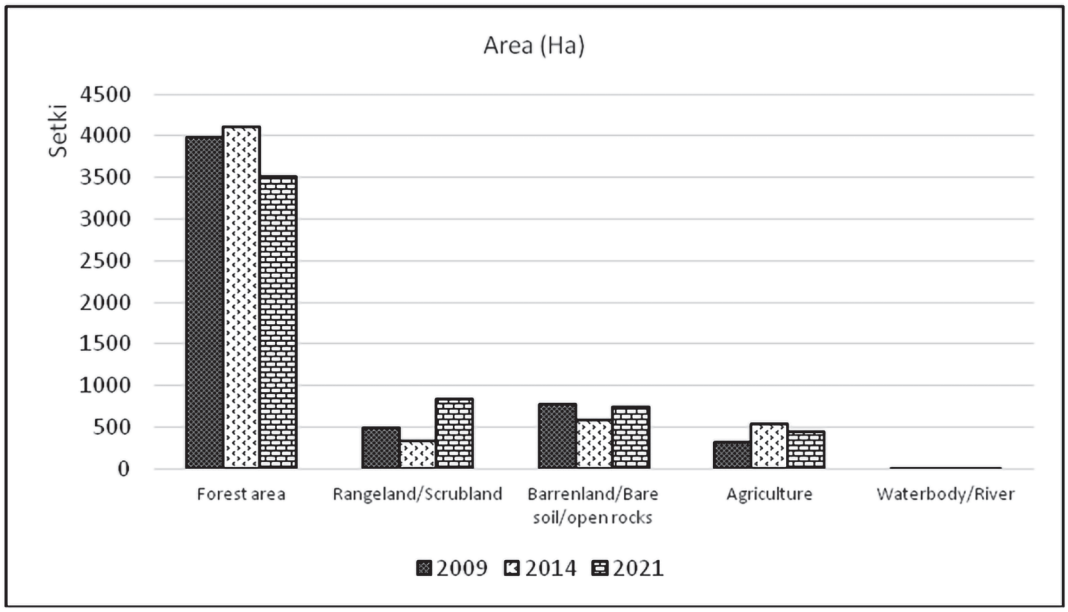

Fig. 6. The LULC classes trend of the years 2009, 2014 and 2021
Ryc. 6. Kierunek zmian w klasach LULC w latach 2009, 2014 i 2021

3.3. Accuracy Assessment of LULC Maps

The accuracy assessment of LULC maps of 2009, 2014, and 2021 has been done using the points collected from the Google Earth from the available high-resolution data sets and following the method of Congallton and Green [41]. The overall accuracy for 2009, 2014, and 2021 are 82%, 86%, and 81% respectively.

3.4. Tehsil Wise Trends of Environmental Factors from the Year 2009 to 2021

3.4.1. Dambuk ADC Tehsil

I. Precipitation

The trend of precipitations shows that the precipitation ranged between 210 and 260 mm from the year 2009 to 2011. In the year 2014 suddenly, precipitation got decreased to 140 mm. From the year 2014 to 2017 the precipitation trend started to increase from the range 130 to 530 mm. From the year 2018 to 2021 the precipitation trend shows decline from 120 to 220 mm.

II. Maximum temperature

The trend of maximum temperature of the upper level shows continuous increase from the year 2009 to 2021 from 25 to 41°C and the trend of maximum temperature at lower end also shows continuous increase from the year 2009 to 2021 from 10 to 16°C.

III. Specific humidity

The trend of specific humidity of the upper end shows continuous increase from the year 2009 to 2017 from 19 to 23 g/kg and the trend of specific humidity at lower end shows continuous decline from the year 2009 to 2016 from 6 to 3 g/kg and the around 3g/kg specific humidity continued up to 2021.

IV. Latent heat flux

The trend of latent heat flux of the upper end from the year 2009 to 2010 ranged from 255 to 276 W/m^2 after the year 2010 trend of latent heat flux of the upper end shows continuous decline up to the year 2021 from 276 to 212 W/m^2. The trend of latent heat flux of the lower end shows small variations from the year 2009 to 2021 from 40 to 10 W/m^2.

V. Sensible heat flux

The trend of sensible heat flux of the upper end from the year 2009 to 2020 shows continuously increasing trend from 90 to 168 W/m^2. In the year 2021 the trend shows sudden decrease i.e. 119 W/m^2 compared to previous year i.e. year 2020. The trend

Table 2. Trends of environmental factors from the year 2009 to 2021
Tabela 2. Kierunki zmian czynników środowiskowych za lata 2009–2021

Tehsil	Environmental Parameter	2009	2011	2014	2017	2019	2021
Dambuk ADC	Precipitation (mm)	8.49	8.36	8.55	9.13	8.51	8.39
	Temp (^{0}C)	23.02	27.58	28.29	29.88	29.67	31.07
	Specific humidity (g/kg)	11.54	10.55	11.41	11.52	11.56	10.94
	Latent heat (W/m^2)	132.73	83.81	93.48	92.69	82.50	67.87
	Sensible heat index (W/m^2)	–38.68	19.28	6.37	14.28	20.16	38.10
Desali circle	Precipitation (mm)	5.35	5.13	5.46	5.66	5.18	5.33
	Temp (^{0}C)	21.62	19.97	22.07	25.31	25.18	25.92
	Specific humidity (g/kg)	10.41	8.39	9.41	9.83	9.83	9.62
	Latent heat (W/m^2)	146.33	96.47	105.51	105.18	94.54	74.63
	Sensible heat index (W/m^2)	–41.83	–0.23	–7.97	–0.50	5.37	29.04
Hunli SDO	Precipitation (mm)	5.81	5.49	5.18	5.64	4.91	4.91
	Temp (^{0}C)	21.62	19.97	22.07	25.31	25.18	25.92
	Specific humidity (g/kg)	10.41	8.39	9.41	9.83	9.83	9.62
	Latent heat (W/m^2)	146.33	96.47	105.51	105.18	94.54	74.63
	Sensible heat index (W/m^2)	–41.83	–0.23	–7.97	–0.506	5.37	29.04
Koronu Circle	Precipitation (mm)	7.77	7.73	7.06	7.70	7.43	6.80
	Temp (^{0}C)	28.45	31.28	30.23	29.83	29.75	30.73
	Specific humidity (g/kg)	11.26	9.56	10.89	10.75	10.65	10.09
	Latent heat (W/m^2)	72.58	50.71	78.24	88.86	73.38	65.46
	Sensible heat index (W/m^2)	57.36	75.53	39.24	27.23	38.42	47.43
Parbuk SDO	Precipitation (mm)	8.43	8.31	8.21	8.82	8.34	8.08
	Temp (^{0}C)	29.55	31.74	30.52	29.88	29.67	31.07
	Specific humidity (g/kg)	12.43	10.45	11.33	11.52	11.56	10.94
	Latent heat (W/m^2)	80.06	56.70	82.89	92.69	82.50	67.87
	Sensible heat index (W/m^2)	39.32	62.05	28.52	14.28	20.16	38.10
Roing HQ	Precipitation (mm)	8.14	8.08	8.14	8.74	8.32	8.12
	Temp (^{0}C)	23.02	28.42	28.72	29.88	29.67	31.07
	Specific humidity (g/kg)	11.54	9.81	11.05	11.52	11.56	10.94
	Latent heat (W/m^2)	132.73	67.96	91.68	92.69	82.50	67.87
	Sensible heat index (W/m^2)	–38.68	43.59	14.11	14.28	20.16	38.10
Tinali Paglam	Precipitation (mm)	9.20	9.10	9.47	9.89	9.67	9.08
	Temp (^{0}C)	29.55	30.35	29.81	29.88	29.67	31.07
	Specific humidity (g/kg)	12.43	11.26	11.72	11.52	11.56	11.43
	Latent heat (W/m^2)	80.06	75.21	86.63	92.69	82.50	67.87
	Sensible heat index (W/m^2)	39.32	34.65	19.41	14.28	20.64	38.10

of sensible heat flux of the lower end continuously shows increase in sensible flux from the year 2009 to 2021 i.e. –170 to –75 W/m^2 .

3.4.2. Desali Circle Tehsil

I. Precipitation

The trend of precipitations shows that the precipitation from the year 2009 to 2013 precipitation got declined from 210 to 90 mm. In the year 2014 suddenly, precipitation got increased up to 330 mm. From the year 2014 to 2021 the precipitation trend started continuously decreasing from the range 330 mm to 160 mm.

II. Maximum temperature

The trend of maximum temperature of upper end shows continuous increase in the years 2009 to 2021 from 31 to 33^{o}C and the trend of maximum temperature at lower end also shows continuous increase in the years 2009 to 2021 from 5 to 18^{o}C.

III. Specific humidity

The trend of specific humidity of the upper end shows slit increase in the years 2009–2021 from 18 to 18.2 g/kg. In-between 2016 and 2017 the trend shows the peak reached up to 19 to 19.1 g/kg. The trend of specific humidity at lower end shows continuous decline from the year 2009 to 2011 from 5 to 2 g/kg and from 2011 to 2021 specific humidity continued 2 g/kg.

IV. Latent heat flux

The trend of latent heat flux of the upper end from the year 2009 to 2020 shows overall decrease from the range 250 to 180 W/m^2. In between the trend of the years 2010, 2014, 2016, 2017 and 2018 shows increased latent heat flux values i.e. 290, 280, 300, 270, 355 W/m^2. The trend of latent heat flux of the lower end shows a small variation from year 2009 to 2012 i.e. from 40 to 20 W/m^2.

V. Sensible heat flux

The trend of sensible heat flux of the upper end of the years 2009–2020 shows continuous increase from 95 to 170 W/m^2. In the year 2021 the trend shows sudden decrease i.e. 120 W/m^2 compared to previous year i.e. 2020. The trend of sensible heat flux of the lower end continuously shows decrease in sensible flux from the year 2009 to 2021 i.e. –160 to –180 W/m^2. In the years 2016 and 2017 the trend shows further lower values i.e. –250 W/m^2.

3.4.3. Hunli SDO Tehsil

I. Precipitation

The trend of precipitations shows that the precipitation was around 130 mm in the year 2009 and in 2010 precipitation got increased up to 178 mm. After 2010 the trend of precipitation shows continuous decline up to the year 2013. In the year 2014 the trend shows the increase in precipitation i.e. around 260 mm. After the year 2014 the trend shows continuous decline in precipitation up to the year 2012 i.e. around 110 mm.

II. Maximum temperature

The trend of maximum temperature of upper end shows a minor variation i.e. 31 to 28^{o}C from the year 2009 to 2013. The trend of maximum temperature at lower end for the year 2009 and 2010 shows around 11^{o}C. From the year 2011 to 2021 trend shows increasing i.e. from 5 to 14^{o}C.

III. Specific humidity

The trend of specific humidity of the upper end shows minor decrease in the years 2009–2013 from 18 to 17 g/kg. The trend shows increase from the year 2014 to 2017 i.e. 18 to 19 g/kg. After the year 2017 the trend started to decline i.e. from 19 to 18 g/ka. The trend of specific humidity at lower end for the years 2009 and 2010 oscillates around 5 g/ka. The trend shows decline in the year 2011 i.e. 2 g/kg and continued up to 2021.

IV. Latent heat flux

The trend of latent heat flux of the upper end in the years 2009–2020 shows overall decrease from 250 to 170 W/m^2. In the year 2012 the trend shows a drastic increase i.e. up to 360 W/m^2. In between the trend of the years 2010, 2014, 2016, 2017 and 2018 shows increased latent heat flux values i.e. 290, 280, 300, 270, 260 W/m^2. The trend of latent heat flux of the lower end shows a small variation from the year 2009 to 2012 i.e. from 40 to 15 W/m^2.

V. Sensible heat flux

The trend of sensible heat flux of the upper end from the year 2009 to 2020 shows continuous increase from 95 to 165 W/m^2 in the year 2021. The trend shows sudden decrease i.e. 126 W/m^2 compared to the previous year i.e. 2020. The trend of sensible heat flux of the lower end continuously shows increase in sensible flux from the year 2009 to 2021 i.e. –167 to –130 W/m^2. In the years 2016 and 2017 the trend shows further lower values i.e. –260 W/m^2.

3.4.4. Koronu Circle Tehsil

I. Precipitation

The trend of precipitations shows that the precipitation was around 240mm in 2009 and in 2010 precipitation increased up to 260mm. After 2010 the trend of precipitation shows continuous decline up to the year 2013. In 2014 the trend shows the increase in precipitation i.e. around 265mm. After 2014 the trend shows continuous decline in precipitation up to 2016, i.e. around 180 mm. In 2017 and 2019 the trend shows the increase in precipitation i.e. 305 and 320 mm. The trend shows that the precipitation decreased in 2020 and 2021 i.e. 140 and 130 mm compared to previous year.

II. Maximum temperature

The trend of maximum temperature of the upper end shows a minor variation i.e. 38 to 36^{o}C from 2009 to 2010. From 2011 the trend shows an increase in maximum temperature i.e. 43^{o}C and further the trend decreased continuously up to 2021 i.e. 40^{o}C. The trend of maximum temperature at lower end for 2009 and 2014 ranged from 18 to 14^{o}C. From 2016 to 2021 the trend shows the increase ranging from 16 to 21^{o}C.

III. Specific humidity

The trend of specific humidity of the upper end shows minor decrease from 2009 to 2011 from 19 to 17 g/kg. The trend shows increase from 2012 to 2017 i.e. 19 to 21 g/kg. After 2017 the trend started to decline i.e. from 21 to 19 g/ka. The trend of specific humidity at lower end for 2009 and 2010 shows around 5 and 4 g/ka. The trend shows decline in the year 2011 i.e. 3 g/kg and continued up to 2021.

IV. Latent heat flux

The trend of latent heat flux of the upper end of 2009 and 2010 is 155 W/m^2 and 190 W/m^2. In 2011 the trend shows further decrease in latent heat flux i.e. up to 100 W/m^2. From 2012 to 2016–17 the latent heat flux increased i.e. from 150 to 230 W/m^2. Further, from the year 2017 to 2020 latent heat flux decreased from 230 to 150 W/m^2. In the year 2021 suddenly, the latent flux heat got increased i.e. 315 W/m^2. The trend of latent heat flux of the lower end shows a small variation from 2009 to 2021, i.e. from 10 to 20 W/m^2.

V. Sensible heat flux

The trend of sensible heat flux of the upper end from 2009 to 2010 decreased i.e. from 150 to 115 W/m^2. In 2011 the trend shows sudden increase in sensible heat flux i.e. 176 W/m^2. After 2011 the sensible heat flux trend started to continuously decline up to the year 2017, i.e. from 176 to 130 W/m^2. For the years 2018, 2019 and 2020 the sensible heat flux values are 170, 155 and 167 W/m^2. In 2021 the trend got decreased i.e. 150 W/m^2 compared to the previous year i.e. year 2020. The trend of sensible heat flux of the lower end continuously shows decrease in sensible flux from 2009 to 2011 i.e. –40 to –148 W/m^2. From 2012 to 2016 the sensible heat flux shows decrease trend i.e. –110 to –170 W/m^2. After the 2016 the trend started to increase up to 2020 i.e. –170 to –95 W/m^2. In 2021 the trend shows decline compared to the previous year i.e. –140 W/m^2.

3.4.5. Parbuk SDO Tehsil

I. Precipitation

The trend of precipitations shows that the precipitation was around 260 mm in 2009 and in 2010 precipitation increased up to 307 mm. After 2010 the trend of precipitation shows continuous decline up to 2013. In 2014 the trend shows the increase in precipitation i.e. around 280mm. After 2014 the trend shows continuous decline in precipitation up to 2016 i.e. around 175 mm. In 2017 and 2019 the trend shows increase in precipitation i.e. 310 and 490 mm. The trend shows that the precipitation decreased in 2020 and 2021 i.e. 190 and 230 mm compared to the previous year.

II. Maximum temperature

The trend of maximum temperature of upper end shows a minor variation i.e. 41 to 37°C from 2009 to 2010. In 2011 the trend shows the increase in maximum temperature i.e. 43°C and further the trend decreased continuously up to 2021 i.e. 41°C. The trend of maximum temperature at lower end for the years 2009 and 2014 ranged from 17 to 14°C. In 2016–2021 the trend shows the increase which ranged from 14 to 21°C.

III. Specific humidity

The trend of specific humidity of the upper end shows minor decrease from 2009 to 2011 from 21 to 19 g/kg. The trend shows the increase from 2012 to 2017 i.e. 21 to 23 g/kg. After 2017 the trend started to decline from 23 to 21 g/ka. The trend of specific humidity at lower end for the years 2009 and 2013 circulates around 5 and 2 g/ka. After 2014 the humidity trend shows the increase from 2 to 3 g/kg.

IV. Latent heat flux

The trend of latent heat flux of the upper end of 2009 and 2010 is 175 W/m^2 and 195 W/m^2. In 2011 the trend shows further decrease in latent heat flux up to 130 W/m^2. From 2012 to 2017 the latent heat flux increased from 160 to 215 W/m^2. Further, from 2018 to 2020 the latent heat flux decreased. from 210 to 175 W/m^2. In 2021, the latent flux heat shows increase i.e. 210 W/m^2. The trend of latent heat flux of the lower end shows a small variation from 2009 to 2021 from 24 to 5 W/m^2.

V. Sensible heat flux

The trend of sensible heat flux of the upper end from 2009 to 2010 decreased from 130 to 70 W/m^2. In 2011 the trend shows sudden increase in sensible heat flux i.e. 170 W/m^2. After 2011 the sensible heat flux trend started to continuously decline up to 2017, i.e. from 170 to 110 W/m^2. For the years 2018, 2019, 2020 and 2012 the sensible heat flux values are 130, 120 and 160 and 165 W/m^2. The trend of sensible heat flux of the lower end continuously shows decrease in sensible flux from the year 2009 to 2016 i.e. –40 to –140 W/m^2. In 2012–2020 the sensible heat flux shows the increasing trend i.e. –140 to –70 W/m^2. In 2021 the trend shows decline compared to the previous year i.e. –110 W/m^2.

3.4.6. Roing HQ Tehsil

I. Precipitation

The trend of precipitations shows that the precipitation was around 280 mm in 2009 and in 2010 precipitation increased up to 330 mm. After 2010 the trend of precipitation shows continuous decline up to 2013 i.e. 150 mm. In 2014 the trend shows increase in precipitation i.e. around 250mm. After 2014 the trend shows continuous decline in precipitation up to 2016 i.e. around 170 mm. In 2017 and 2019 the trend shows increase in precipitation i.e. 330 and 300 mm. The trend shows that precipitation decreased in 2020 and 2021, i.e. 200 and 170 mm compared to previous year.

II. Maximum temperature

The trend of maximum temperature of the upper end shows a minor variation i.e. 33 to 31°C from 2009 to 2010. From 2011 trend shows there was an increase in maximum temperature i.e., 41°C, and further the trend continued up to 2021 i.e. 41°C. The trend of maximum temperature at lower end for the year 2009 and 2010 ranged from 11 to 9°C. From 2010 to 2021 the trend shows the increase, which ranged from 9 to 21°C.

III. Specific humidity

The trend of specific humidity of the upper end shows minor decrease from the year 2009 to 2011 from 19 to 17 g/kg. The trend shows increase from 2012 to 2017 i.e. 19 to 22 g/kg. After 2017 trend started to decline i.e. from 22 to 21 g/ka up to the year 2021. The trend of specific humidity at lower end for the years 2009 and 2014 shows around 5 and 2 g/ka. After 2014 the humidity trend shows increase from 2 to 5 g/kg.

IV. Latent heat flux

The trend of latent heat flux of the upper end of the year 2009 and 2010 is 260 W/m^2 and 270 W/m^2. In 2011 the trend shows further decrease in latent heat flux i.e. up to 140 W/m^2. In 2012 the latent heat flux got increased i.e. 190. In 2013 the latent heat further increased up to 240 W/m^2. Further, from 2013 to 2021 the latent heat flux decreased i.e. from 240 to 210 W/m^2. The trend of latent heat flux of the

lower end shows small variation from 2009 to 2021 i.e. from 30 to 10 W/m^2.

V. Sensible heat flux

The trend of sensible heat flux of the upper end from 2009 to 2011 increased i.e. from 90 to 170 W/m^2. After 2011 the sensible heat flux trend started to continuously decline up to 2021 i.e. from 170 to 110 W/m^2. The trend of sensible heat flux of the lower end continuously shows decrease in sensible flux from the year 2009 to 2013 i.e. –170 to –190 W/m^2. After the years 2013–2020 the sensible heat flux shows the increase trend i.e. –190 to –70 W/m^2. In 2021 the trend shows decline compared to the previous year i.e. –113 W/m^2.

3.4.7. Tinali Paglam Circle Tehsil

I. Precipitation

The trend of precipitations shows that the precipitation was around 200mm in 2009 and in 2010 precipitation increased up to 350 mm. After 2010 the trend of precipitation shows continuous decline up to 2014 i.e. 200mm. Increase in precipitation is seen for the years 2015, 2017 and 2019 i.e. 230, 370 and 530 mm. Between 2016 and 2018 there was less precipitation i.e. 200 and 210 mm. After 2019 the precipitation trend shows decline for 2020 and 2021 i.e. 260 and 264 mm.

II. Maximum temperature

The trend of maximum temperature of the upper end shows a minor variation i.e. 42 to 37°C from 2009 to 2010. From 2011 to 2021 the trend shows a decrease in maximum temperature i.e. from 42 to 41°C. The trend of maximum temperature at lower end for the year 2009 and 2010 ranged from 17 to 13°C. From 2010 to 2021 the increasing trend was observed ranging from 13 to 21°C.

III. Specific humidity

The trend of specific humidity of the upper end shows minor decrease from 2009 to 2011 from 21 to 20 g/kg. The trend shows increase from 2012 to 2017 i.e. 20 to 22 g/kg. After 2017 the trend started to decline i.e. from 22 to 21 g/ka up to 2021. The trend of specific humidity at lower end for 2009 and 2013 shows around 5 and 2 g/ka. After 2013 the humidity trend shows increase from 2 to 5 g/kg up to 2021.

IV. Latent heat flux

The trend of the latent heat flux of the upper end of 2009 and 2010 is 170 W/m^2 and 190 W/m^2. In 2011 the trend shows further decrease in latent heat flux i.e. up to 160 W/m^2. From 2012 to 2013 the latent heat flux increased from 200 to 240 W/m^2. In 2014 the latent heat decreased up to 190 W/m^2. From the year 2015 the latent heat flux decreased up to the year 2021 i.e. from 235 to 210 W/m^2. The trend of latent heat flux of the lower end shows a small variation from 2009 to 2021 i.e. from 20 to 10 W/m^2.

V. Sensible heat flux

The trend of sensible heat flux of the upper end from 2009 to 2010 decreased i.e. from 130 to 90 W/m^2. From 2011 to 2012 latent heat flux shows the increasing trend i.e. 135 to 140 W/m^2. From 2012 the sensible heat flux trend shows continuous decline till 2017 i.e. from 140 to 110 W/m^2. After 2017 the sensible heat flux trend started to increase from 110 to 170 W/m^2. The trend of sensible heat flux of the lower end continuously shows decrease in sensible flux from 2009 to 2016 i.e. –45 to –140 W/m^2. After 2016 till 2021 the sensible heat flux shows increase i.e. –140 to –60 W/m^2.

4. DISCUSSION

4.1 Decadal Change on Lulc

The decrease in forest area and increase of scrub/rangeland and agriculture suggest there was a demand for a new settlement that reduced the forest cover. The population increase from 2009 to 2021 was the main driving force that affected the reduction in forest area including the clearing of big trees for timber and wood extraction for fuel. This finds support from the previous works in the region [31–33]. The increase in urban areas contributes significantly to the loss of vegetation/forest cover, accelerating carbon emission [38, 39]. This would also increase surface temperature and global warming. According to some study [12] vegetation cover loss increases temperature by 11°C in 25 years, the maximum temperature increases in industrial zone. Further it was found that poor vegetation ra-

diates high temperature while healthy vegetation radiates low temperature [12]. Tree-based systems with healthy vegetation cover can minimize radiation and store more carbon [27]. Population growth and changes in per capita consumption of food, fodder, fibre, timber and energy is on the rise in the region resulting in continued land use changes [27, 29, 33]. The rapid expansion of build-up areas followed by loss of green cover is drastically impacting the carbon sink potential of various land uses and increasing climate hazards. Conversion of crop lands often leads to losses in food production and additional risk to food systems in the fragile mountain landscape. To mitigate climate hazards sustainable land management is highly essential. Efforts should therefore be made to slow down urbanization to reduce pollution gateways and to improve carbon sink potential through afforestation, and other eco-friendly inclusive and sustainable urban development. The indigenous communities that largely depend on forest resources for their livelihoods could be sensitized to promote sustainable biodiversity conservation through judicious land-use management that can also stabilize carbon dioxide accumulation at the local and regional level and help to mitigate climate change in the region [40].

As per the global forest watch (https://www.global-forestwatch.org/) report, the total forest area of Lower Dibang Valley in the year 2010 was 396000 ha which is 71% of the total area and in 2020 the total forest area got decreased by 745 ha. Our findings also match the total forest area estimations and the total percentage covered by the global forest watch results. High fire alerts were reported between the 2nd of November 2020 and the 25th of October 2021 for the forests of this region. This is unusually high compared to previous years going back to 2012. Between the 29th of October 2018 and the 25th of October 2021, the Lower Dibang Valley experienced a total of 221 VIIRS fire alerts. The forest fire seems to be the one the main reasons for the decrease in the forest area. The mountainous and sloping topographic structure of the region, complex vegetation of the area and negative climate conditions are the essential reasons for those difficulties. For this reason, it was quite hard to find usable (not cloudy) satellite images. Some other problems had stemmed from using different sensor technologies (spatial resolution and spectral resolution) in comparing Landsat TM and Landsat 8 data, and in the determination of land cover. These problems were tried to be eliminated by independently applying the supervised classification change detection technique to all 3 date images.

5. CONCLUSIONS

This paper investigated land use/land cover changes that occurred in the Lower Dibang valley between 2009, 2014, and 2021 using remote sensing and GIS. The main change observed between 2009 and 2021 was that the area of forest decreased from 398 472.8 ha to 351 590.8 ha i.e. from 71% of total forest area in 2009 to 63% in 2021 while the total forest area decreased by 8%. The significant change in forest cover has led to loss of various ecosystem services including loss of carbon stock from these land uses. The major impact has been occurred on climatic and environmental variables i.e. precipitation got decreased, maximum temperature got increased. The major driver for this change was due to expansion of infrastructure in recent years. It is therefore suggested that the policy makers, urban planners and local governments should implement eco-friendly, inclusive and sustainable urban development by modifying the degraded landscape through tree-based and agroforest systems for better livelihood and environmental sustainability.

DISCLOSURES

The authors declare that they have no competing interests.

ACKNOWLEDGMENTS

The authors are thankful to all the reviewers for their valuable comments and suggestions which have helped for the overall improvement of the quality of the research paper.

REFERENCES

1. Rawart, J.S., Biswas, V., Kumar, M. Changes in land use/cover using geospatial techniques: A case study of Ramnagar town area, district Nainital, Uttarakhand, India. Egypt J Remote Sens Space Sci., 2013; volume 16, pp. 111–117.
2. Kumar, M., Arup, D., Richa, S., Supratik, S. Change detection analysis using multi-temporal satellite data of Poba reserve forest, Assam and Arunachal Pradesh. Int. J. GeomatGeosci. 2014; volume 4, pp. 517–527.

3. Lambin, E.F., Turner, B.L., Geist, H.J., Agbola, S.M., Angelsen, A., Bruce, J.W., Coomes, O.T., Dirzo, R., Fischer, G., Folke, C. The causes of land-use and land-cover change: Moving beyond the myths. Glob. Environ Chang, 2011, volume 11, pp. 261–269.
4. Al-Kafy, A., Saha, M., Al-Faisal, A., Rahaman, Z., Rahman, M.T., Liu, D., Fatteh, M.A., Rakib, A.A., Al-Doubari, A.E., Rahaman, S.N., Hasan, M.Z., Ahasan, M.A.K. Predicting the impact of land use/land cover changes on seasonal urban thermal characteristics using maching learning algorithms. Build Environ (https://doi.org/10.1016/j.buildenv.2022.109066), 2022; volume 217.
5. Ritse, V., Basumatary, H., Kulnu, A.S., Dutta, G., Phukan, M.M., Hazarika, N. Monitoring land use land cover changes in the Eastern Himalayan landscape of Nagaland, Northeast India. Environ Monit Assess. 2020; volume 192(11), pp. 1–17.
6. Emiru, B., Ashfare, H., Fenta, A.A., Hishe, H., Gebremedhin, M.A., Wahed, H.G., Solomon, N. Land use land cover changes along topographic gradients in Hugumburda national forest priority area, Northern Ethiopia. Remote SensApplSoc Environ, 2018, volume 13, pp. 61–6.
7. Sankhala, S., Singh, B. Evaluation of urban sprawl and land use/land cover change using remote sensing and GIS techniques: A case study of Jaipur City, India. Int. J. Emerg. TechnolAdvEng. 2014; volume 4, pp. 66–72.
8. Hegazy, I.R., Mosbeh, R.K. Monitoring urban growth and land use change detection with GIS and remote sensing technique in Daqahlia governorate Egypt. Int. J. Sustain Built Environ, 2015; volume 4, pp. 117–124.
9. Chomitz, K.M., Kamari, K. The domestic benefits of tropical forests. World Bank Res Obs. 1998; volume 13, pp. 13–35.
10. Bruijnzeel, L.A. Hydrological functions of tropical forests: Not seeing the soil for the trees? AgricEcosyst Environ. 2004, volume 104, pp. 185–228.
11. Cheruto, M.C., Kauti, M.K., Kisangau, P.D., Kariuki, P. Assessment of land use and land cover change using GIS and remote sensing techniques: A case study of Makueni County, Kenya. J Remote Sens GIS. 2016; volume 5, pp. 175.
12. Al-Kafy, A., Al-Faisal, A., Rakib, A.A., Fattah, M.A., Rahaman, Z.A., Sattar, G.S. Impact of vegetation cover loss on surface temperature and carbon emission in a fastest growing cities, Cumilla, Bangladesh. Build Environ (https://doi.org/j.buildenv.2021.108573). 2022b; volume 208.
13. Minale, A.S. Retrospective analysis of land cover and use dynamics in GilgelAbbay Watershed using GIS and remote sensing technique, Northwestern Ethiopia. Int. J. Geosci. 2013, volume 4, pp. 1003–1008.
14. Meshesha, T.W., Tripathi, S.K., Khare, D.M. Analyses of land use and land cover change dynamics using GIS and remote sensing during 1984 and 2015 in the Beressa Watershed Northern Central Highland of Ethiopia. Model Earth Syst. Environ. 2016; volume 2, pp. 1–12.
15. Adeel, M. Methodology for identifying urban growth potential using land use and population data: A case study of Islamabad Zone IV. Procedia Environ Sci. 2010; volume 2, pp. 32–41.
16. Rawart, J.S., Kumar, M. Monitoring land use/cover change using remote sensing and GIS techniques: A case of Hawallbagh block, district Almora, Utterkland, India. Egypt J. Remote Sens Space Sci. 2015, volume 18, pp. 77–84.
17. Weng, Q. A remote sensing-GIS evaluation of urban expansion and its impacts on the temperature in the Zhujiang Delta, China. Int. J. Remote Sens. 2011; volume 22, 1999–2014.
18. Hassan, Z., Rabia, S., Sheikh, A., Amir, H.M., Neelam, A., Amna, B., Summra, E. Dynamics of land use and land cover change (LULCC) using geospatial techniques: A case study of Islamabad Pakistan. Springer Plus. 2016; volume 5, pp. 812.
19. Liang, S., Fang, H., Morisette, J.T., Chen, M., Shuey, C.J., Walthall, C.L., Daughtry, C.S. Atmospheric correction of Landsat ETM+ Land surface imagery. II. Validation and applications. IEEE Trans Geosci Remote Sens. 2022; volume 4, pp. 2736–2746.
20. Ayele, G.T., Demessie, S.S., Mengistu, K.T., Tilahun, S.A., Melesse, A.M. Multitemporal land use/land cover change detection for the Batena Watershed, Rift Valley Lakes Basin, Ethiopia. In: Landscape Dynamics, Soils and Hydrological Processes in Varied Climates; Springer: Berlin, Germany, 2016; pp. 51–72.
21. Lambin, E.F., Geist, H.J. Global land-use and land-cover change: What have we learned so far. Glob Chang Newsl. 2001; volume 46, pp. 27–30.
22. Woldeamlak, B. Land covers dynamics since the 1950s in Chemoga Watershed, Blue Nile Basin, Ethiopia. Mt Res Dev. 2002; volume 22, pp. 263–269.
23. Manandhar, R., Odeh, I.O., Ancev, T. Improving the accuracy of land use and land cover classification of Landsat data using post-classification enhancement. Remote Sensing. 2009; volume 1(3), pp. 330–344.
24. Alshari, E.A., Gawali, B.W. Development of classification system for LULC using remote sensing and GIS. Global Transitions Proceedings. 2021, volume *2*(1), pp. 8–17.
25. Negi, V.S., Pathalk, R., Rawal, R.S., Bhatta, I.D., Sharma, S. Long term ecological monitoring of forest ecosystems in Indian Himalayan region: Criteria and indicator approach. Ecol Indic. 2019; volume 102, pp. 374–381.
26. Nath, A.J., Kumar, R., Devi, N.B., Rocky, P., Giri, K., Sahoo, U.K., Bajpai, R.K., Sahu, N., Pandey, R. Agroforestry land suitability analysis in the eastern Himalayan region. Environ Chall (doi: 10.1016/j.envc.2021.100199), 2021.
27. Singh, S.L., Sahoo, U.K., Gogoi, A., Kenye, A. Effect of land use changes on carbon stock dynamics in major land use sectors of Mizoram, Northeast India. J Environ Prot. 2018; volume 9, pp. 1262–1285.
28. Sahoo, U.K., Singh, S.L., Gogoi, A., Kenye, A., Sahoo, S.S. Active and passive soil organic carbon pools as affected by different land use types in Mizoram, Northeast India. PLoS One. 2019; volume 14(7).
29. Ahirwal, J., Nath, A., Brahma, B., Deb, S., Sahoo, U.K., Nath, A.J. Pattern and driving factors of biomass carbon and soil organic carbon stock in the Indian Himalayan region. Sci. Total Environ. 2021; volume 770.
30. Thong, P., Pebam, R., Sahoo, U.K. A geospatial approach to understand the dynamics of shifting cultivation in Champhai

district of Mizoram. North-east India. J. Indian Soc Remote Sensdoi, 2018.
31. Thong, P., Sahoo, U.K., Pebam, R., Thangjam, U. Spatial and temporal dynamices of shifting cultivation in Manipur, Northeast India based on time-series satellite data. Remote Sens Appl Soc Environ. 2019a; volume 14, pp. 126–137.
32. Thong, P., Sahoo, U.K., Pebam, R., Thangjam, U. Changing trends of shifting cultivations and its drivers in Champhai, Northeast India. Ind. J. Hill Farm. 2019b; volume 32(1), pp. 1–4.
33. Gogoi, A., Sahoo, U.K. Impact of anthropogenic disturbances on species diversity and vegetation structure of a lowland tropical rainforest of eastern Himalaya, India. J. Mount Sci. 2018; volume 15(11), pp. 2453–2465.
34. CBD Conference of Parties to Convention on Biological Diversity. Fourteenth Meeting Item 21 of the Provisional Agenda. Sharm EI-Sheikh, Egypt, November 2018, pp. 17–29.
35. Gogoi, A., Ahirwal,, J., Sahoo, U.K. Plant biodiversity and carbon sequestration potential of the planted forest in Brahmaputra flood plains. J. Environ Manage (10.1016/j.envman.2020.111671), 2021.
36. Deka, J., Tripathi, O.P., Khan, M.L., Srivastava, V.K. Study on land-use and land-cover change dynamics in eastern Arunachal Pradesh, NE India using remote sensing and GIS. Trop Ecol. 2019; volume 60, pp. 199–208.
37. Areendran, G., Raj, K., Majumdar, S., Joshi, R., Puri, K. Land use land cover mapping of Mouling National Park in Arunachal Pradesh, India using geospatial tools. International J. Science Environment. 2018; volume 7(2), pp. 696–705.
38. Sahoo, U.K., Tripathi, O.P., Nath, A.J., Deb, S., Das, D.J., Gupta, A., Devi, N.B., Chaturvedi, S.S., Singh, S.L., Kumar, A., Tiwari, B.K. Quantifying tree diversity, carbon stocks and sequestration potential for diverse land-uses in northeast India. Front Env. Sci. (https://doi.org/10.3389/fenvs.2021.724950), 2021.
39. Bordoloi, R., Das, B., Tripathi, O.P., Sahoo, U.K., Nath, A.J., Deb, S., Das, D.J., Gupta, A., Devi, N.B., Chaturvedi, S.S., Tiwari, B.K., Paul, A., Tajo, L. Satellite based integrated approaches to modeling spatial carbon stock and carbon sequestration potential of different land uses of northeast India. Environ Sust Indic (https://doi.org/100166, https://doi.org/10.1016/j.indic.2021.100166). 2022, volume 13:
40. Deb, D., Jamatia, M., Debbarma, J., Ahirwal, J., Deb, S., Sahoo, U.K. Evaluating the role of community-managed forest in carbon sequestration and climate change mitigation of Tripura, India. Air Water Soil Pollut (https://doi.org/10.1007/s11270-021-05133-z). 2021, volume 232, pp. 166.
41. Congallton, R.G., Green, K. Assessing accuracy of remote sensed data. Remote Sensing Environment. 1999, volume 37, pp. 35–46.
42. Sari, H., Ozsahin, E. Spatiotemporal change in the LULC (Landuse/Landcover) characteristics of Tekirdag Province based on the CORINE (Thrace, Türkiye). Fresenius Environ Bull. 2016, volume 25, pp. 4694–4707.
43. Ikiel, C., Dutucu, A.A., Ustaoglu, B., Kilic, D.E. Land use and land cover (LULC) classifcation using Spot-5 image in the Adapazari Plain and its surroundings, Türkiye. TOJSAT Online J. Sci. Technol. 2012; volume 2, pp. 37–42.
44. Yilmaz, Y.A., Sen, O.L., Turuncoglu, U.U. Modeling the hydroclimatic efects of local land use and land cover changes on the water budget in the upper Euphrates – Tigris basin. J. Hydrol. (https://doi.org/10.1016/j.jhydrol.2019.06.074). 2019; volume 576, pp. 596–609.
45. Xie, Q., Sun, Q. Monitoring the spatial variation of aerosol optical depth and its correlation with land use/land cover in Wuhan, China: a perspective of urban planning. Int. J. Environ Res Public Health (https://doi.org/10.3390/ijerph18031132). 2021, volume 18, pp. 1–18.
46. Kharol, S.K., Kaskaoutis, D.G., Badarinath, K.V.S. Influence of land use/land cover (LULC) changes on atmospheric dynamics over the arid region of Rajasthan state, India. J. Arid Environ (https://doi.org/10.1016/j.jaridenv.2012.09.006). 2013, volume 88, pp. 90–101.
47. Liou, Y.A., Kar, S.K. Evapotranspiration estimation with remote sensing and various surface energy balance algorithms-a review. Energies (https://doi.org/10.3390/en7052821). 2014; volume 7, pp. 2821–2849.
48. Xie, Q., Sun, Q. Monitoring the spatial variation of aerosol optical depth and its correlation with land use/land cover in Wuhan, China: a perspective of urban planning. Int. J. Environ Res Public Health (https://doi.org/10.3390/ijerph18031132). 2021; volume 18, pp. 1–18.
49. Achugbu, I.C., Olufayo, A.A., Balogun, I.A. Modeling the spatiotemporal response of dew point temperature, air temperature and rainfall to land use land cover change over West Africa. Model Earth Syst. Environ (ttps://doi.org/10.1007/s40808-021-01094-8). 2022; volume 8, pp. 173–198.
50. Zadbagher, E., Becek, K., Berberoglu, S. Modeling land use/land cover change using remote sensing and geographic information systems: case study of the Seyhan Basin, Türkiye. Environ Monit Assess (https://doi.org/10.1007/ s10661-018-6877-y). 2018; volume 190, pp. 494.
51. Karimi, P., Bastiaanssen, W.G.M. Spatial evapotranspiration, rainfall and land use data in water accounting – part 1: review of the accuracy of the remote sensing data. Hydrol. Earth Syst. Sci. (https://doi.org/10.5194/hess-19-507-2015). 2015; volume 19, pp. 507–532.
52. Zhang, Y., Balzter, H., Wu, X. Spatial-temporal patterns of urban anthropogenic heat discharge in Fuzhou, China, observed from sensible heat fux using Landsat TM/ETM+ data. Int. J. Remote Sens (https://doi.org/10.1080/01431161.2012.718465). 2013; volume 34, pp. 1459–1477.
53. Wang, X.G., Wang, W., Huang, D., Yong, B., Chen, X. Modifying SEBAL model based on the trapezoidal relationship between land surface temperature and vegetation index for actual evapotranspiration estimation. Remote Sens (https://doi.org/10.3390/rs60x000x). 2014; volume 6, pp. 5909–5937.